Published in final edited form as:
Circ Res. 2009 July 17; 105(2): 201–208. doi:10.1161/CIRCRESAHA.109.196790.

Angiomodulin is a specific marker of vasculature and regulates VEGF-A dependent neo-angiogenesis

Andrea T. Hooper[1], **Sergey V. Shmelkov**[1], **Sunny Gupta**[2], **Till Milde**[1], **Kathryn Bambino**[1], **Kelly Gillen**[1], **Mollie Goetz**[1], **Sai Chavala**[1], **Muhamed Baljevic**[1], **Andrew J. Murphy**[3], **David M. Valenzuela**[3], **Nicholas W. Gale**[3], **Gavin Thurston**[3], **George D. Yancopoulos**[3], **Linda Vahdat**[4], **Todd Evans**[2,5], and **Shahin Rafii**[1]

[1]Howard Hughes Medical Institute, Department of Genetic Medicine, Ansary Stem Cell Institute, Weill Cornell Medical College, 1300 York Avenue, New York, New York, 10065

[2]Department of Developmental & Molecular Biology, Albert Einstein College of Medicine, Bronx, New York, 10461

[3]Regeneron Pharmaceuticals, 777 Old Saw Mill River Road, Tarrytown, New York, 10591

[4]Department of Medicine, Weill Cornell Medical College, 1300 York Avenue, New York, New York, 10065

Abstract

Blood vessel formation is controlled by the balance between pro- and anti-angiogenic pathways. Although much is known about the factors that drive sprouting of neovessels, the factors that stabilize and pattern neovessels are undefined. The expression of angiomodulin (AGM), a VEGF-A binding protein, was increased in the vasculature of several human tumors as compared to normal tissue, raising the hypothesis that AGM may modulate VEGF-A-dependent vascular patterning. To elucidate the expression pattern of AGM, we developed an AGM knockin reporter mouse ($AGM^{lacZ/+}$) wherein we demonstrate that AGM is predominantly expressed in the vasculature of developing embryos and adult organs. During physiological and pathological angiogenesis, AGM is upregulated in the angiogenic vasculature. Using the zebrafish model, we found that AGM is restricted to developing vasculature by 17-22 hpf. Blockade of AGM activity with morpholino oligomers (MO) results in prominent angiogenesis defects in vascular sprouting and remodeling. Concurrent knockdown of both AGM and VEGF-A results in synergistic angiogenesis defects. When VEGF-A is overexpressed, the compensatory induction of the VEGF-A receptor, VEGFR-2/flk-1, is blocked by the simultaneous injection of AGM MO. These results demonstrate that the vascular-specific marker AGM modulates vascular remodeling in part by temporizing the pro-angiogenic effects of VEGF-A.

Keywords

Angiomodulin; IGFBP-7; angiogenesis; VEGF; zebrafish

Corresponding Author: Shahin Rafii, MD Howard Hughes Medical Institute Weill Cornell Medical College 1300 York Ave, Room A-863 New York, NY 10021, USA Tel: 212 746 2070 Fax: 212 746 8481 srafii@med.cornell.edu.
[5]Current Address: Department of Surgery, Weill Cornell Medical College, 1300 York Avenue, New York, NY 10065.

DISCLOSURES: None.

INTRODUCTION

The development of blood vessels is modulated by the balance between pro- and anti-angiogenic factors. Vascular endothelial growth factor-A (VEGF-A) via signaling through its cognate receptors VEGFR2 and VEGFR1 modulates destabilization, proliferation, invasion and sprouting of neovessels, orchestrating the formation of neovasculature. The expression of factors that temporize the potent effects of VEGF-A is necessary to facilitate the remodeling of nascent neovessels into functional vasculature. Although it is known that thrombospondins (TSPs), angiopoietins and soluble VEGFR1 have roles in vessel stabilization, unrecognized matrix-associated factors may regulate the effects imparted by VEGF-A.

Among the known matrix-bound factors, angiomodulin (AGM) is implicated in cell adhesion, endothelial cell (EC) biology and tumor progression, however, its function in developmental and pathogenic angiogenesis is unknown.[1-4] AGM is secreted by ECs, smooth muscle cells (SMCs) and fibroblasts, and is predominantly localized to the extracellular matrix (ECM).[5, 6] AGM binds chemokines and growth factors, including VEGF-A and is deposited on vascular basement membranes in tumor tissues and in high endothelial venules and may serve as a biochemical growth factor reservoir.[5-7] Tumor ECs reportedly express AGM, although the expression pattern is complicated by the fact that tumor cells may express AGM. Nevertheless, the expression of AGM during embryogenesis, adulthood and tumorigenesis and function during embryogenesis is unknown.

The architecture of the vascular system is defined by vasculogenesis and angiogenesis. In zebrafish, vasculogenesis results in the formation of the longitudinal axial vessels, the dorsal aorta (DA) and posterior cardinal vein (PCV).[8-10] Angiogenesis is responsible for the formation of the remaining vasculature network, including intersomitic vessels (ISV), which sprout from axial vessels in a temporally predictable manner.[11] Therefore, it has been proposed that there are designated sites for branching and initial pathway guidance for ISVs, although precise mechanisms are unknown.[11] Migratory and proliferative ECs respond to pro- and anti-angiogenic signals from adjacent tissues, modify ECM interactions, and form new blood vessels that undergo extensive remodeling.[10] VEGF-A is required for ISV outgrowth from the DA In that zebrafish treated with low-doses of VEGF-A morpholino oligomers (MO) form the DA but do not form ISVs.[12] Even so, it is unclear what angiogenic modulators act with VEGF-A to choreograph the initial positioning and subsequent patterning of the sprouts.

To uncover the mechanism by which AGM regulates neoangiogenesis, we determined AGM expression during development and in adults, both at steady state and during tumorigenesis. We interrogate the function of AGM during zebrafish embryogenesis and demonstrate that AGM, via interaction with VEGF-A, is critical for the formation of neovessels.

METHODS

Human tissue

This study was conducted according to the principles expressed in the Declaration of Helsinki. Human tissues were obtained from patients who provided informed consent, as approved by and in accordance with the Institutional Review Boards of Weill Cornell Medical College (WCMC) and Memorial Sloan Kettering Cancer Center.

Animals & generation of AGM$^{lacZ/+}$ knock-in mice

C57BL/6 mice were obtained from Jackson Laboratories. AGM$^{lacZ/+}$ knockin mice were generated by high-throughput VelociGene technology.[13] Animal experiments were performed with authorization from the Institutional Animal Care and Use Committee of WCMC using age- and sex-matched animals.

Detection of β-galactosidase activity in mouse tissues

For standard detection of β-gal, soft tissues from AGM$^{lacZ/+}$ mice were frozen in OCT. Femurs were fixed in PFA, decalcified in 10% EDTA and snap-frozen in OCT. For enhanced detection animals were perfused with PBS, then 0.2% glutaraldehyde (GA), followed by 4 hour post-fix. All tissues were cryosectioned, fixed for 10 min in 0.2% GA, incubated with X-gal overnight (1mg/ml, Calbiochem), then counterstained with Nuclear Fast Red (NFR, Vector Labs).

Histology

Frozen sections of human or mouse tissue were blocked and incubated in anti-AGM antibodies followed by appropriate polyclonal secondary antibody (Jackson IR) and streptavidinhorseradish peroxidase (Jackson IR). Staining was developed with AEC+ or DAB + (DAKO). Serial sections were stained in Mayer's hematoxylin (DAKO) and/or eosin (H&E, Richard-Allan Scientific).

Models of angiogenesis

Abdominal skin of AGM$^{lacZ/+}$ mice was surgically opened, sutured, and allowed to heal. Five days post-surgery skin was harvested for X-gal staining. For the tumor model, 1×10^6 LLC cells were injected subcutaneously on the flank of AGM$^{lacZ/+}$ mice and allowed to develop. On day 21 tumors were harvested for X-gal staining. For oxygen induced retinopathy (OIR) model, postnatal day (P) 7 AGM$^{lacZ/+}$ pups were exposed to 75% oxygen for 5 days, and at P12 were placed in room air. P17 retinas were whole-mounted, co-stained with GS-IB4 isolectin (Vector) and anti-β-gal Ab (ICN/Cappel) and were counterstained with ToPro-3 (Invitrogen). For the myelosuppression model, 250 mg/kg 5-fluorouracil (5-FU) was administered on Day 0 via intravenous tail vein injection (i.v.). Mice were allowed to recover and tissues were harvested for X-gal staining at indicated timepoints.

Fish stocks and maintenance

Zebrafish embryos were maintained at 28°C and staged as described.[14] Unless otherwise specified, experiments utilized embryos derived from parents of a hybrid strain (ABTU) obtained by breeding AB and TU strains (Zebrafish International Research Center/ZIRC). Tg (*fli1*:EGFP) line was obtained from the ZIRC. Embryos were collected, raised and staged in embryo medium until they reached the desired developmental stage.

Reverse Transcription (RT), PCR and quantitative PCR (qPCR)

Total RNA extracted from embryos, adult zebrafish and tumor tissues using Trizol (Invitrogen) followed by DNase I treatment (Promega) underwent cDNA synthesis with Superscript-II (Invitrogen). PCR was performed using Advantage2 Polymerase (BD Biosciences) and these primers: AGM Fwd: 5'-GTGGAACATCACTGGATCTC-3'; AGM Rev: 5'-CTCGCTGTCCTTCACCATC-3' (amplicon length: 328bp; annealing temperature: 60°C; elongation time: 30s; number of cycles: 35;); EF1α Fwd: 5'-CTTCTCAGGCTGACTGTGC-3'; EF1α. Rev: 5'-CCGCTAGCATTACCCTCC-3' (300bp; 60°C; 30s; 25 cycles). qPCR was performed using Power SYBR green on ABI 7500 Fast System (Applied Biosystems). qPCR conditions were 50°C for 2 minutes and 95°C for 10 minutes, then 40 cycles of 95°C for 15 seconds and 60°C for 1 minute. Primers were designed using Primer Express Software v. 3.0 (Applied Biosystems): EF1α Fwd: 5'-CCCCTCCGTCTGCCACTT-3', EF1α Rev: 5'-CCACACGACCCACAGGTACA-3'; AGM Fwd: 5'-GGCGGCCCCGAGAA-3', AGM Rev: 5'-TTTAGTGAGCGGTGAGATCAGAAC-3'. Data were analyzed with SDS software v. 1.3.1 (Applied Biosystems). Relative quantification was determined using the delta Ct method: relative expression = $(2^{-\text{delta Ct}})*10000$.

Whole-mount in situ hybridization

Whole mount in situ hybridization was performed essentially as described[15]. Digoxigenin-labeled RNA antisense probe for AGM was generated by using the following PCR primers to clone a 450 bp fragment of AGM from the I.M.A.G.E. clone 6969595: Fwd 5'-ATGCTGTGTGTTCTCGTCCT-3', Rev 5'-GATGTTCCACACCTCTCCTG-3'. The PCR fragment was ligated into pCR4-TOPO vector (Invitrogen) and digested with NotI for antisense probe synthesis and PmeI for sense probe synthesis. T3 and T7 were used for antisense and sense probe synthesis, respectively. Two-color whole-mount in situ hybridization was performed as described previously, although instead of Fast Red, INT Red (Sigma) was used to develop the red color. Fluorescein-12-UTP-labeled GFP probe and digoxigenin-labeled AGM probe were hybridized simultaneously.

Antisense morpholino oligomers

Morpholino oligomers (MO) were synthesized by GeneTools LLC (Philomath, OR): AGM-ATG-MO (translational blocking antisense, ATG-MO), 5'-GGCGAGGACGAGAACACACAGCATG; AGM-SPL-MO (splicing antisense, SPL-MO), 5'-CATCCAGAGCTGCTCACCCTGCGCG; and VEGF-MO (translational blocking antisense, VEGF-MO), 5'-GTATCAAATAAACAACCAAGTTCAT. Various non-specific MOs were used as controls.

VEGF-A Overexpression

VEGF-A_{165} and VEGF-A_{121} RNA were transcribed & capped *in vitro* using mMessage mMachine *in vitro* transcription kit (Applied Biosystems/Ambion). Capped RNA was poly-A tailed using Poly(A) Tailing Kit (Applied Biosystems/Ambion). 100 pg of VEGF-$A_{165/121}$ in a 1:1 ratio was injected into 1-2 cell zebrafish embryos. In experiments where AGM antisense MOs were used, ATG-MOs were co-injected with VEGF-$A_{165/121}$ RNA. 24 hours post fertilization (hpf), RNA was isolated and cDNA was reverse transcribed. flk1 qPCR was performed using the following primers: flk-1 fwd: 5'-CACAAGAAGTCCAGCGATCA-3'; flk-1 rev: 5'-CAGGGGACCACAAAATATGG-3'. Data were analyzed for relative quantification.

Imaging

Brightfield images were captured an Olympus BX51 (Olympus) with an AxioCam digital camera (Zeiss). Fluorescence and transmitted light images were captured on a Discovery stereomicroscope (Zeiss). Confocal images were taken and analyzed on a LSM 510 Meta confocal microscope (Zeiss).

RESULTS

AGM is increased in the vasculature of human tumors

AGM protein localized to tumor vasculature of invasive breast carcinoma, glioblastoma, and lymphoma tumor samples (Figure 1A-F). AGM was observed in perivascular stromal cells and was robustly expressed at the leading edge of invasive breast carcinoma (Figure 1D). In contrast, minimal AGM expression was found in vasculature of either normal adjacent breast tissue or breast reduction specimens (Figure 1C arrows, data not shown). In sections from metastatic colon carcinoma in the liver, normal liver and border areas between malignant and normal tissue, we found increased AGM expression in vasculature of the primary tumor and tumor-normal border zone (Figure 1G-H) as compared to normal adjacent liver (Figure 1I). These results demonstrate that AGM is upregulated in human tumor vasculature.

AGM is predominantly expressed by smooth muscle invested vasculature in adults

We generated a knock-in mouse (AGM$^{lacZ/+}$) whereby the AGM native promoter drives β-galactosidase (β-gal) expression. We observed AGM promoter activity in the vasculature of all organs at steady state (Figure 2A, Online Figure IIA). Using standard methods, β-gal reporter activity was predominantly localized to the SMC-invested large vessels with lesser expression in capillaries (Figure 2A). Using immunohistochemistry, AGM protein was localized to the vasculature or collagen type IV-rich compartments (Figure 2B, Online Figure IIB, data not shown). When β-gal was detected with a high sensitivity protocol, AGM expression demarcated virtually all vasculature, except liver and bone marrow (BM) where it was expressed at low levels. Therefore, AGM$^{lacZ/+}$ mice may be used as a vascular specific reporter mouse model (Online Figure IIA).

AGM is upregulated during angiogenesis

In order to delineate the expression of AGM during pathologic angiogenesis we performed tumor growth, wound healing, hypoxia and myelosuppression studies. We detected AGM immunoreactivity in the uterus (Figure 3A). When Lewis Lung Carcinoma (LLC) cells were injected subcutaneously into AGM$^{lacZ/+}$ mice to form tumors, β-gal activity was concentrated at the tumor leading edge and in the vasculature (Figure 3A, dotted line). The induction of a skin wound in the abdomen of AGM$^{lacZ/+}$ mice resulted in upregulated β-gal activity in the angiogenic vasculature within granulation tissue of regenerating skin (Figure 3A). In AGM$^{lacZ/+}$ mice subjected to OIR model of angiogenesis, we used co-immunofluorescence to detect β-gal protein with endothelial specific GS-IB4 isolectin. AGM was upregulated in neoangiogenic tufts (Figure 3A, arrows). In steady state BM, AGM is expressed by SMC-invested arterioles (Figure 2A). In the 5-FU model of hemangiogenesis, where myelosuppression causes an angiogenic response in BM sinusoids, AGM expression was upregulated in sinusoidal ECs after myelosuppression (Figure 3B). qPCR of whole BM confirmed these results (data not shown). In order to investigate the expression of AGM during embryogenesis we harvested AGM$^{lacZ/+}$ embryos different stages of embryonic development and stained for β-gal activity (Figure 3C, Online Figure IIA-I). AGM was expressed by 10.5 days post-coitus, increased in intensity throughout embryogenesis, and was restricted to the vasculature (Figure 3C-N). These data indicate that AGM is upregulated selectively in remodeling neovessels during both pathologic and embryonic angiogenesis suggesting that AGM might play a role in modulating neo-angiogenesis.

Identification of AGM in zebrafish

In order to define the function of AGM *in vivo*, we employed the zebrafish model. Because the vasculature of the zebrafish trunk is patterned and develops in a regular array it is an excellent model for the study of angiogenesis. We used amino acid sequences of murine and human *agm* genes to search for a zebrafish orthologue of AGM. Zebrafish *agm* is localized to chromosome 14 and consists of five exons. A corresponding full-sized zebrafish cDNA clone (I.M.A.G.E. 6969595; Accession #BC067677) was obtained and sequenced. The predicted protein contains 257 amino acids with 50 and 54% homology to mouse and human AGM, respectively (Online Figure IIIA, Supplemental Table 1). Examination of the predicted protein domain structure using InterProScan program on EMBL-EBI demonstrates that zebrafish AGM consists of a conserved cysteine-rich IGFBP domain, a Kazal-type serine proteinase inhibitor domain and an immunoglobulin cell adhesion molecule domain, similar to the protein structure of mammalian AGM (Figure 4A). Zebrafish AGM is phylogenetically closest to that of rainbow trout IGFBP7 (Online Figure IIIB, Online Table I). Similar to its orthologues in other species, zebrafish AGM has only modest homology (7-22% overall) to the other previously identified members of the zebrafish IGFBP superfamily and the homologous region is localized to the IGFBP domain where the homology is from 25-44% (Online Table II).[16]

AGM expression is stage- and tissue-specific, and localized to the vasculature during zebrafish embryogenesis

Using whole mount *in situ* hybridization (ISH) to examine the expression of AGM during zebrafish embryogenesis, we detected AGM mRNA by 17 hpf localized to the medial floor plate of the neural tube (Figure 4B-C, blue arrows). By 22-24 hpf AGM mRNA was also detected in the DA and the newly forming ISV (Figure 4B, C, yellow arrows). Embryos of various stages stained with sense riboprobes were negative for signal demonstrating antisense probe specificity (Figure 4B, inset). By 28-48 hpf AGM transcripts were detected in the vasculature of the head, eye and trunk (Figure 4B). Double ISH experiments with a probe specific for the vasculature demonstrated that AGM transcripts were in the vascular endothelium (Figure 4C). We then performed RT-PCR and qPCR analyses for AGM on whole embryos, and observed that AGM mRNA was present at low levels immediately after the pregastrula period at 10 hpf and transcript levels increased as long as 48 hpf (Figure 4D-E). RT-PCR and qPCR showed that AGM mRNA is robustly expressed in skeletal muscle and eye of adult fish and to a lesser extent in other tissues examined (Figure 4F-G).

Knockdown of AGM using morpholinos results in a multi-factorial phenotype consistent with angiogenic defects

We used the morpholino antisense knockdown approach to test the function of AGM during vascular development (Figure 5). We designed two MOs specific for AGM: one targeting the 5' UTR through the first 25 bases of coding sequence which inhibits translation (ATG-MO) and the other targeting a splice junction at the first coding exon-intron boundary (SPL-MO). In order to assess specificity of the MOs to inhibit AGM transcription, we used RT-PCR and qPCR and showed a significant decrease in AGM transcript levels at 24 hpf after the injection of 20 ng SPL-MO into fertilized eggs (Figure 5A). Notably, equivalent embryonic phenotypes were found by injection of ATG-MO, which blocks AGM expression by a different mechanism (Online Table III). These data confirm that antisense MOs, which target AGM specifically and efficiently, suppress the translation of AGM mRNA into functional protein.

Embryos injected with either 2.5-10 ng of ATG-MO or 10ng of the SPL-MO exhibited delayed embryonic development and a multi-factorial phenotype (Figure 5B, Online Table III). Injection of either MO resulted in reduced anterior-posterior length, delayed or reduced pigmentation, and cardiovascular defects (Figure 5B, Online Table III). Defects in cardiovascular development became evident in the AGM morphants between 22-25 hpf, coincident with the onset of blood circulation. Embryos injected with either ATG-MO or SPL-MO exhibited a visible reduction or absence of circulating blood cells at 28 and 48 hpf (Online Table III). Largely reduced or absent blood flow through ISVs, formed via angiogenic sprouting from the DA, was observed in embryos derived from ATG-MO or SPL-MO injected fertilized eggs, suggestive of a defect in angiogenesis (Online Table III). In addition, the development of pericardial edema was observed in the majority of morphants injected with either MO (Figure 5B, Online Table III).

Knockdown of AGM disrupts vascular development during zebrafish embryogenesis

The defects in circulation and the pericardial edema indicates that knockdown of AGM compromises the development of vascular tissues. To monitor this process *in vivo*, we knocked down AGM expression in *fli1*:EGFP zebrafish vascular reporter embryos (Figure 5C-E). Although, as mentioned above, there was a defect in axial circulation in many embryos due to a reduction in hematopoiesis, we detected no gross defects to primary vasculogenesis in AGM morphant embryos (Online Table III, Figure 5C-E). However, examination of secondary vascular structures revealed vascular patterning defects in regions where AGM mRNA expression was observed. Specifically, angiogenic sprouting of ISV from the DA was impaired and mispatterned in fertilized eggs injected with either ATG-MO or SPL-MO (Figure 5C-E,

Online Table IV, Online Movie I). The resulting morphants had reduced protrusive activity and ISV sprout length, as compared to controls (Figure 5C-E, Online Table IV, Online Movie I). By 48 hpf, there was noticeable failure of the ISV to extend properly to the DLAV in morphant embryos. Detailed analysis showed that the majority of the AGM morphants exhibited partial to complete loss of ISV patterning, compared with 100% of the control embryos showing normal establishment of ISV sprouting from the DA to the DLAV (Figure 5C-E, Online Table IV). These data indicate that vascular expression of AGM during early embryonic development regulates the patterning of the developing vessels.

AGM interacts with the VEGF-A pathway

The AGM loss-of-function phenotype is strikingly similar to the phenotype of VEGF-A knockdown in zebrafish embryos.[12] VEGF-A morphants develop blood vessel deficiencies with wide-ranging phenotypes.[12] Phenotypes can range from partial loss of ISV, when MOs are injected at low dose, to a complete loss of ISV accompanied by a pericardial edema and blood accumulation in the ventral trunk at high dose. *In vitro* studies have shown that VEGF-A binds AGM, although the physiological consequence of this interaction is unknown.[5] The similarity in phenotypes between AGM and VEGF-A morphants suggests that AGM and VEGF-A may share common angiogenic pathways.

To test this hypothesis, we compared the pattern and extent of angiogenesis in *fli1*:EGFP embryos injected with either AGM-specific ATG-MO or VEGF-MO, alone or in combination. MO-mediated knockdown of both VEGF-A and AGM together revealed a synergistic effect on angiogenesis in zebrafish embryos, strongly supporting a genetic interaction (Figure 6A-G). At a subeffective dosage of either ATG-MO or VEGF-MO alone, there was little overall effect on angiogenesis. However, simultaneous knockdown of both VEGF-A and AGM at these same doses significantly inhibited and disrupted angiogenic sprouting of ISV from the DA (Figure 6AG, Online Movies II & III). In addition, significant arterio-venous shunts, loss of circulation with or without blood accumulation in the trunk was observed in a significant number of double MO embryos (Figure 6G, data not shown). Thus, compared with single MO-based knockdown of each gene, double knockdown of VEGF-A and AGM resulted in a statistically significant phenotypical shift to severe vascular defects, suggesting that VEGF-A interacts *in vivo* with AGM.

In order to explore the role of the interaction of the VEGF pathway with AGM, we overexpressed VEGF-A, via injection of VEGF-$A_{165/121}$ mRNA into fertilized eggs, resulting in the compensatory upregulation of the VEGF-A receptor-2 (flk-1).[17] We found that when VEGF-A is overexpressed in the presence of AGM-specific ATG-MO we were able to abrogate the effects of VEGF-A overexpression on flk-1 upregulation (Figure 6H), suggesting that AGM lies upstream in the VEGF-A signaling pathway. Taken together, these data implicate that the interaction between AGM and VEGF-A is critical for proper neovessel remodeling during zebrafish development and that AGM may act upstream of VEGF-A signaling during angiogenic sprouting.

DISCUSSION

We have employed genetic tracking studies in mice and loss-of-function studies in zebrafish to examine the role of the AGM during vascular development. Although AGM has been implicated to play a role in tumorigenesis, the functional role of AGM in physiological neoangiogenesis has not been studied.[18] Herein, we show that during embryonic development and in adult mice, AGM expression is restricted to the vasculature and upregulated during neoangiogenic processes. In order to interrogate the function of AGM, we identified a zebrafish orthologue of AGM and demonstrated that AGM performs as an angiogenic factor patterning the blood vasculature during embryogenesis via temporization of VEGF-A activity.

AGM is expressed by and is largely localized to human tumor vasculature and is not ubiquitous in the vasculature normal tissues. In the AGM reporter mice, AGM is upregulated during angiogenesis, but is also detectable in the vessels of normal tissues. The ability to detect AGM in normal mouse tissues is likely due to sensitivity of β-gal enzymatic staining. Therefore, it is probable that AGM is expressed at low levels in the normal human vasculature but is upregulated during tumorigenesis.

In addition, we observed robust expression of AGM during murine embryogenesis and its expression was localized to the vasculature. To study the physiological relevance of AGM expression during embryogenesis, we utilized the zebrafish model. We found a previously undescribed zebrafish orthologue of AGM that is highly expressed in the DA and the vasculature of the head and ISVs, which form via angiogenesis. Furthermore, AGM is expressed in many adult zebrafish tissues – particularly the eye and skeletal muscle, corroborating the expression data from the AGM reporter mouse model. Therefore, AGM may be used to selectively identify blood vessels during embryonic development and in adult organs. To define the function of AGM in angiogenesis, we employed the zebrafish *fli1*:EGFP model. Injections of *fli1*:EGFP zebrafish with two different MOs resulted in loss-of-function embryos with similar angiogenic phenotypes. The DA and CV, formed via vasculogenesis, were largely normal, however, angiogenic sprouts from axial vessels were absent, reduced or mispatterned – suggesting that during embryogenesis AGM is a pro-angiogenic factor critical for proper patterning of ISVs. The vascular defect appears to represent a developmental delay rather than a complete block in angiogenesis, which might be explained by the fact that AGM is not expressed in the CV from where secondary angiogenic sprouts arise.

VEGF-A is critical for the molecular patterning of the embryonic vasculature[12] and it was demonstrated previously that VEGF-A binds to AGM.[5] We demonstrate a genetic interaction between VEGF-A and AGM because MOs targeting both VEGF-A and AGM transcripts, when administered simultaneously at subeffective doses, resulted in a robust and reproducible abrogation of angiogenesis. Moreover, AGM MOs are able to abrogate the effects of VEGF-A overexpression, suggesting that AGM acts upstream of VEGF-A. Collectively, these data support a model wherein AGM may provide for an extracellular scaffold to which VEGF-A can bind within the ECM milieu resulting in the proper downstream signaling and guidance of nascent angiogenic vasculature. Most likely the binding of VEGF-A to the ECM bound AGM might prevent excessive bioavailability of VEGF-A thereby allowing for proper vascular patterning. In support of this notion, we also demonstrate that AGM is robustly expressed by the vasculature of tumors suggesting that AGM, by modulating VEGF-A pro-angiogenic activity, may promote the formation of functional non-leaky neo-vessels.

The data herein dictate a novel role for AGM in modulation of growth factor bioavailability and as a modulator of the angiogenic switch. Whether AGM behaves as a proangiogenic factor may depend on the regional composition of the ECM microenvironment. Indeed, other factors, including TGF-β and TSPs recruited and deposited into the ECM have been shown to modulate neoangiogenesis and temporize the effects of proangiogenic factors, including FGFs and VEGFs. In conclusion, AGM is an evolutionarily conserved marker of developing and adult vasculature. AGM is overexpressed during pathogenic angiogenesis and functions as a proangiogenic factor in the developing vasculature, in concert with VEGF-A and potentially other angiogenic factors, patterning and stabilizing neovessels. We speculate that increasing AGM levels through enhanced delivery of VEGF-A will accelerate neoangiogenesis, while blocking AGM will diminish the aberrant overgrowth of VEGF-A dependent vessels. Further investigation is necessary to elucidate additional partners of AGM that may function collaboratively during embryogenesis and angiogenesis.

Supplementary Material

Refer to Web version on PubMed Central for supplementary material.

Acknowledgments

We thank Audrey Holtzinger and Lisa McReynolds (Einstein) for their expertise in zebrafish techniques. Excellent fish husbandry was provided by Spartak Kalinin (Einstein).

SOURCES OF FUNDING

This work was supported by the Howard Hughes Medical Institute, Ansary Stem cell Institute, National Heart, Lung and Blood Institute (P50 HL084936), Anbinder and Paul Newman Foundation and New York State Dept. of Health, NYS C023042 (S.R.). T.E. and S.R. are supported by the National Institutes of Health (TE: R01 grants HL056182 and HL064282; S.R.: R01 grants HL075234, HL059312 and R21HL083222-02).

REFERENCES

1. Sato J, Hasegawa S, Akaogi K, Yasumitsu H, Yamada S, Sugahara K, Miyazaki K. Identification of cell-binding site of angiomodulin (AGM/TAF/Mac25) that interacts with heparan sulfates on cell surface. J Cell Biochem 1999;75:187–195. [PubMed: 10502291]
2. Yamauchi T, Umeda F, Masakado M, Isaji M, Mizushima S, Nawata H. Purification and molecular cloning of prostacyclin-stimulating factor from serum-free conditioned medium of human diploid fibroblast cells. Biochem J 1994;303:591–598. [PubMed: 7980422]
3. Swisshelm K, Ryan K, Tsuchiya K, Sager R. Enhanced expression of an insulin growth factor-like binding protein (mac25) in senescent human mammary epithelial cells and induced expression with retinoic acid. Proc Natl Acad Sci U S A 1995;92:4472–4476. [PubMed: 7538673]
4. Murphy M, Pykett MJ, Harnish P, Zang KD, George DL. Identification and characterization of genes differentially expressed in meningiomas. Cell Growth Differ 1993;4:715–722. [PubMed: 7694637]
5. Usui T, Murai T, Tanaka T, Yamaguchi K, Nagakubo D, Lee CM, Kiyomi M, Tamura S, Matsuzawa Y, Miyasaka M. Characterization of mac25/angiomodulin expression by high endothelial venule cells in lymphoid tissues and its identification as an inducible marker for activated endothelial cells. Int Immunol 2002;14:1273–1282. [PubMed: 12407018]
6. Akaogi K, Okabe Y, Sato J, Nagashima Y, Yasumitsu H, Sugahara K, Miyazaki K. Specific accumulation of tumor-derived adhesion factor in tumor blood vessels and in capillary tube-like structures of cultured vascular endothelial cells. Proc Natl Acad Sci U S A 1996;93:8384–8389. [PubMed: 8710880]
7. Nagakubo D, Murai T, Tanaka T, Usui T, Matsumoto M, Sekiguchi K, Miyasaka M. A high endothelial venule secretory protein, mac25/angiomodulin, interacts with multiple high endothelial venule-associated molecules including chemokines. J Immunol 2003;171:553–561. [PubMed: 12847218]
8. Vogeli KM, Jin SW, Martin GR, Stainier DY. A common progenitor for haematopoietic and endothelial lineages in the zebrafish gastrula. Nature 2006;443:337–339. [PubMed: 16988712]
9. Stainier DY, Weinstein BM, Detrich HW 3rd, Zon LI, Fishman MC. Cloche, an early acting zebrafish gene, is required by both the endothelial and hematopoietic lineages. Development 1995;121:3141–3150. [PubMed: 7588049]
10. Fouquet B, Weinstein BM, Serluca FC, Fishman MC. Vessel patterning in the embryo of the zebrafish: guidance by notochord. Dev Biol 1997;183:37–48. [PubMed: 9119113]
11. Childs S, Chen JN, Garrity DM, Fishman MC. Patterning of angiogenesis in the zebrafish embryo. Development 2002;129:973–982. [PubMed: 11861480]
12. Nasevicius A, Larson J, Ekker SC. Distinct requirements for zebrafish angiogenesis revealed by a VEGF-A morphant. Yeast 2000;17:294–301. [PubMed: 11119306]
13. Valenzuela DM, Murphy AJ, Frendewey D, Gale NW, Economides AN, Auerbach W, Poueymirou WT, Adams NC, Rojas J, Yasenchak J, Chernomorsky R, Boucher M, Elsasser AL, Esau L, Zheng J, Griffiths JA, Wang X, Su H, Xue Y, Dominguez MG, Noguera I, Torres R, Macdonald LE, Stewart AF, DeChiara TM, Yancopoulos GD. High-throughput engineering of the mouse genome coupled with high-resolution expression analysis. Nat Biotechnol 2003;21:652–659. [PubMed: 12730667]

14. Westerfield, M. The zebrafish book : a guide for the laboratory use of zebrafish (Brachydanio rerio). 2.1. ed.. Eugene, OR., editor. Distributed by the Institute of Neuroscience, University of Oregon; M. Westerfield: 1994.

15. Alexander J, Stainier DY, Yelon D. Screening mosaic F1 females for mutations affecting zebrafish heart induction and patterning. Dev Genet 1998;22:288–299. [PubMed: 9621435]

16. Hwa V, Oh Y, Rosenfeld RG. The insulin-like growth factor-binding protein (IGFBP) superfamily. Endocr Rev 1999;20:761–787. [PubMed: 10605625]

17. Liang D, Chang JR, Chin AJ, Smith A, Kelly C, Weinberg ES, Ge R. The role of vascular endothelial growth factor (VEGF) in vasculogenesis, angiogenesis, and hematopoiesis in zebrafish development. Mech Dev 2001;108:29–43. [PubMed: 11578859]

18. Wajapeyee N, Serra RW, Zhu X, Mahalingam M, Green MR. Oncogenic BRAF induces senescence and apoptosis through pathways mediated by the secreted protein IGFBP7. Cell 2008;132:363–374. [PubMed: 18267069]

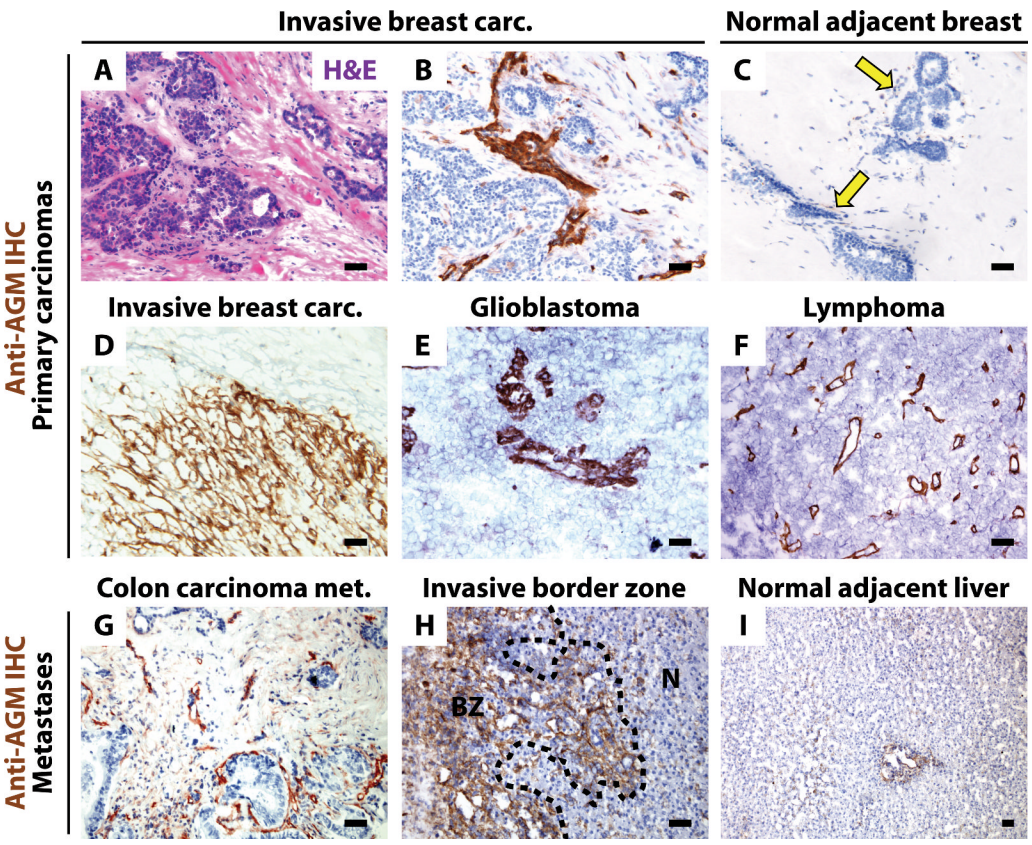

Figure 1. AGM is localized to tumor vasculature in human carcinomas

A-I) Human tumor and normal adjacent tissues were stained with H&E (A) or anti-AGM antibody (B-I). Invasive breast carcinoma (A-B) shows vascular-associated AGM. AGM is minimal in normal adjacent breast (arrows). (C). Invasive breast carcinoma leading edge expresses AGM (D). Glioblastoma (E) and lymphoma (F) vasculature expresses AGM. Metastatic colon carcinoma expresses AGM in the tumor vasculature (G). AGM is robustly positive at the border zone (BZ) between tumor and normal adjacent liver (N) (H). Normal adjacent liver expresses minimal AGM (I). *Micron bar = 50 μm.*

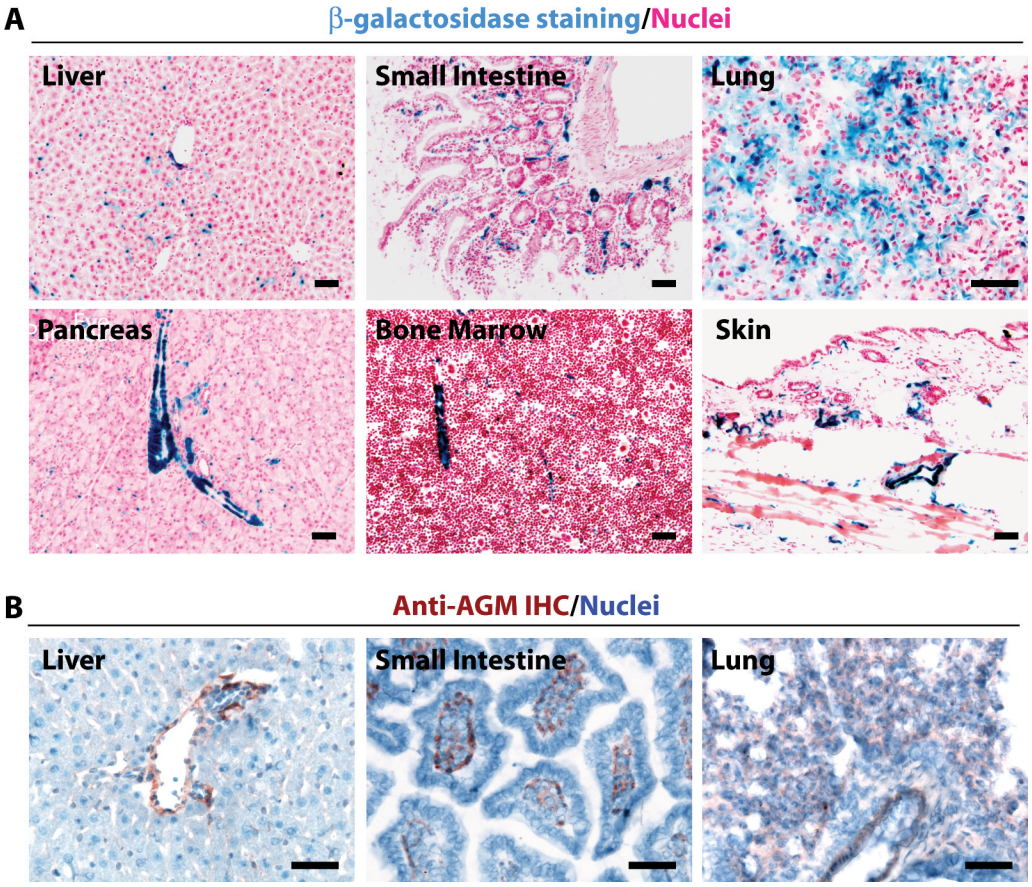

Figure 2. AGM expression is restricted to the adult vasculature

A) AGM$^{lacZ/+}$ organs were stained for β-gal activity (blue). AGM is largely restricted to the vasculature and predominates in SMC-invested large vessels in small intestine, lung, pancreas, bone marrow, and skin, with little staining in liver. B) Tissues from C57BL/6 mice were immunostained for AGM (red/brown). AGM is weakly expressed in vascular rich tissues. *Micron bar = 50 μm.*

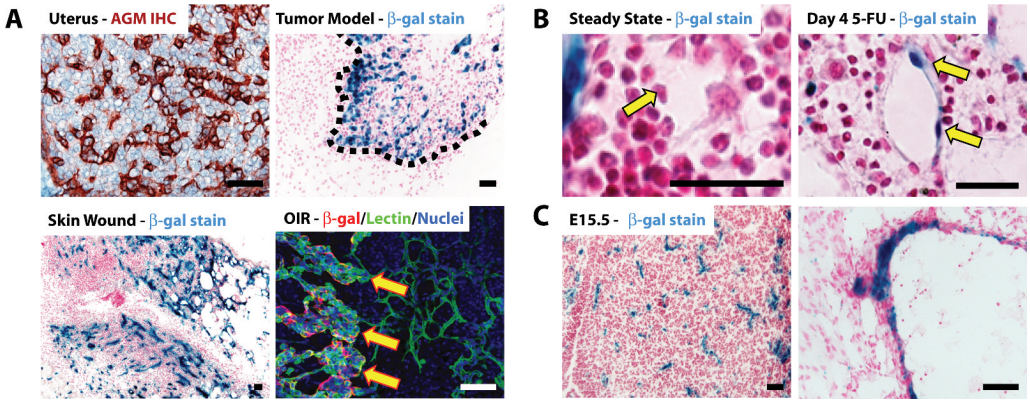

Figure 3. AGM expression is restricted to the vasculature during embryonic development and is upregulated during neoangiogenesis

AGM expression was assessed during neoangiogenesis. A) IHC detection of AGM (brown) in C57BL/6 uterus shows robust AGM expression. AGM$^{lacZ/+}$ mice were injected subcutaneously with LLC tumor cells and monitored for tumor formation. Tumors were stained for β-gal activity (blue). AGM is preferentially expressed in tumor vasculature at the leading edge (dotted line). Detection of β-gal activity in skin wounds in AGM$^{lacZ/+}$ mice. Skin was injured and the wound tissue was harvested at 5 days. Tissue sections were stained for β-gal activity (blue). AGM expression is increased in the regenerating angiogenic skin. Oxygen-induced retinopathy (OIR) model of pathologic neoangiogenesis. Retinas were harvested from AGM$^{lacZ/+}$ mice, whole-mounted and stained with GS-IB4 isolectin (green) and anti-β-gal Ab (red). AGM (red) is increased in neoangiogenic tufts (arrows). *Micron bar = 50 μm.* B) AGM$^{lacZ/+}$ mice were injected i.v. with 5-FU and allowed to recover. BM was harvested at day 4 for β-gal activity (blue). AGM is upregulated in the angiogenic sinusoidal ECs (arrow) during hemangiogenic recovery. *Micron bar = 20 μm.* C) Sections of AGM$^{lacZ/+}$ embryos at E15.5 were stained for β-gal activity (blue) demonstrating AGM expression in the vasculature. *Micron bar = 50 βm.*

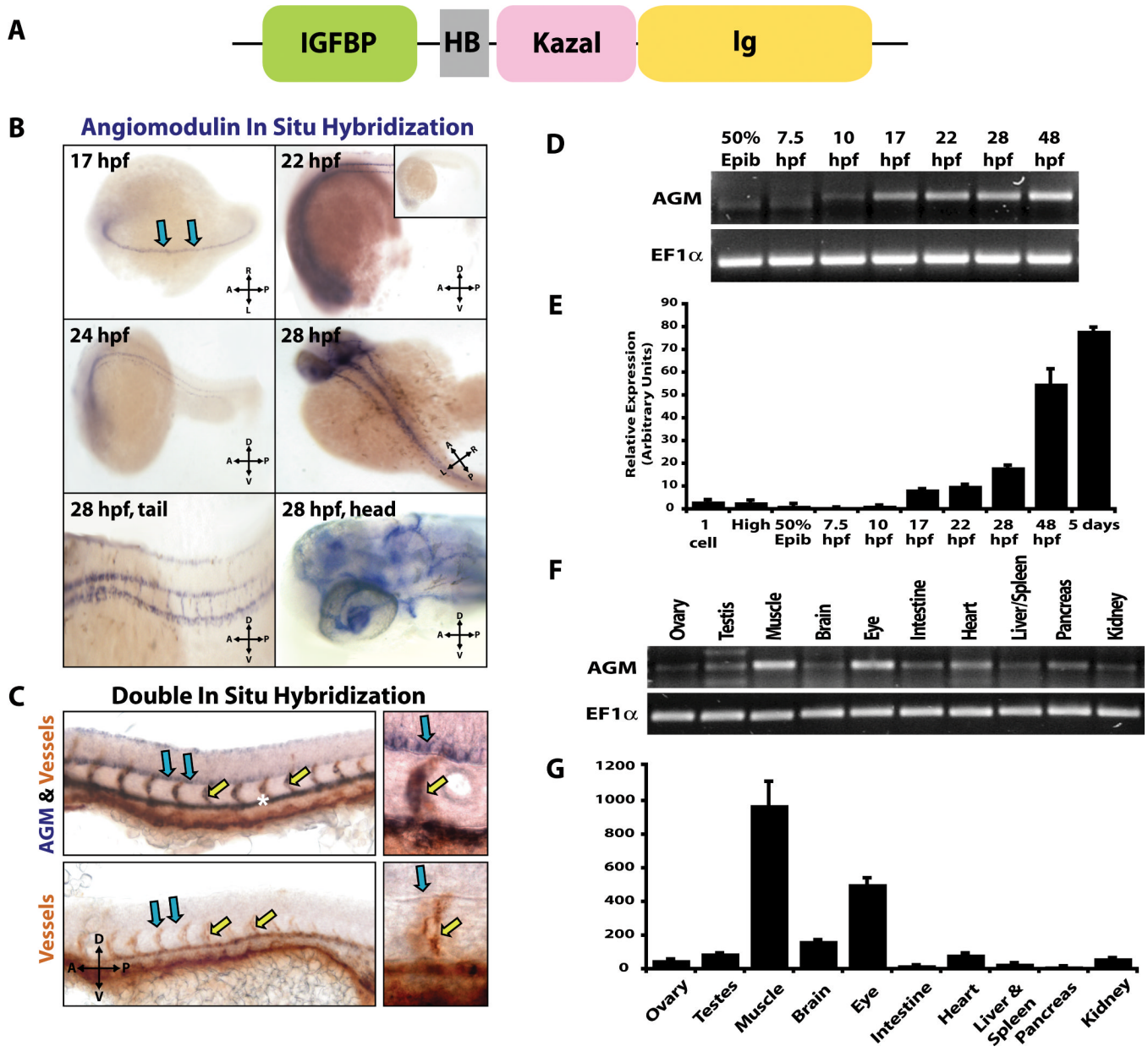

Figure 4. AGM is expressed by the developing vasculature during zebrafish embryogenesis

A) Predicted domain structure of zebrafish AGM protein. B) ABTU embryos were hybridized with antisense probes for AGM (blue): 17 hpf antisense – AGM transcripts in the medial floor plate of the neural tube (blue arrows); 22 hpf antisense & 24 hpf antisense – AGM transcripts are in medial floor plate and DA (inset – sense control); 28 hpf whole body, tail and head antisense – AGM transcripts are in ISVs and vasculature of the head. C) *fli1*:EGFP fish were co-hybridized with AGM specific riboprobe (blue) and GFP specific riboprobe for detection of vasculature (orange). AGM is expressed in the DA (asterisk), ISVs (yellow arrows) and medial floor plate (blue arrows). Sense probe co-hybridized with GFP riboprobe is shown in bottom two panels. D-E) RT-PCR (D) and qPCR (E) for AGM on total RNA from 30-100 ABTU embryos at various developmental stages. F-G) RT-PCR (F) and qPCR (G) for AGM on total RNA extracted from adult tissues harvested from ABTU zebrafish. *n=3*.

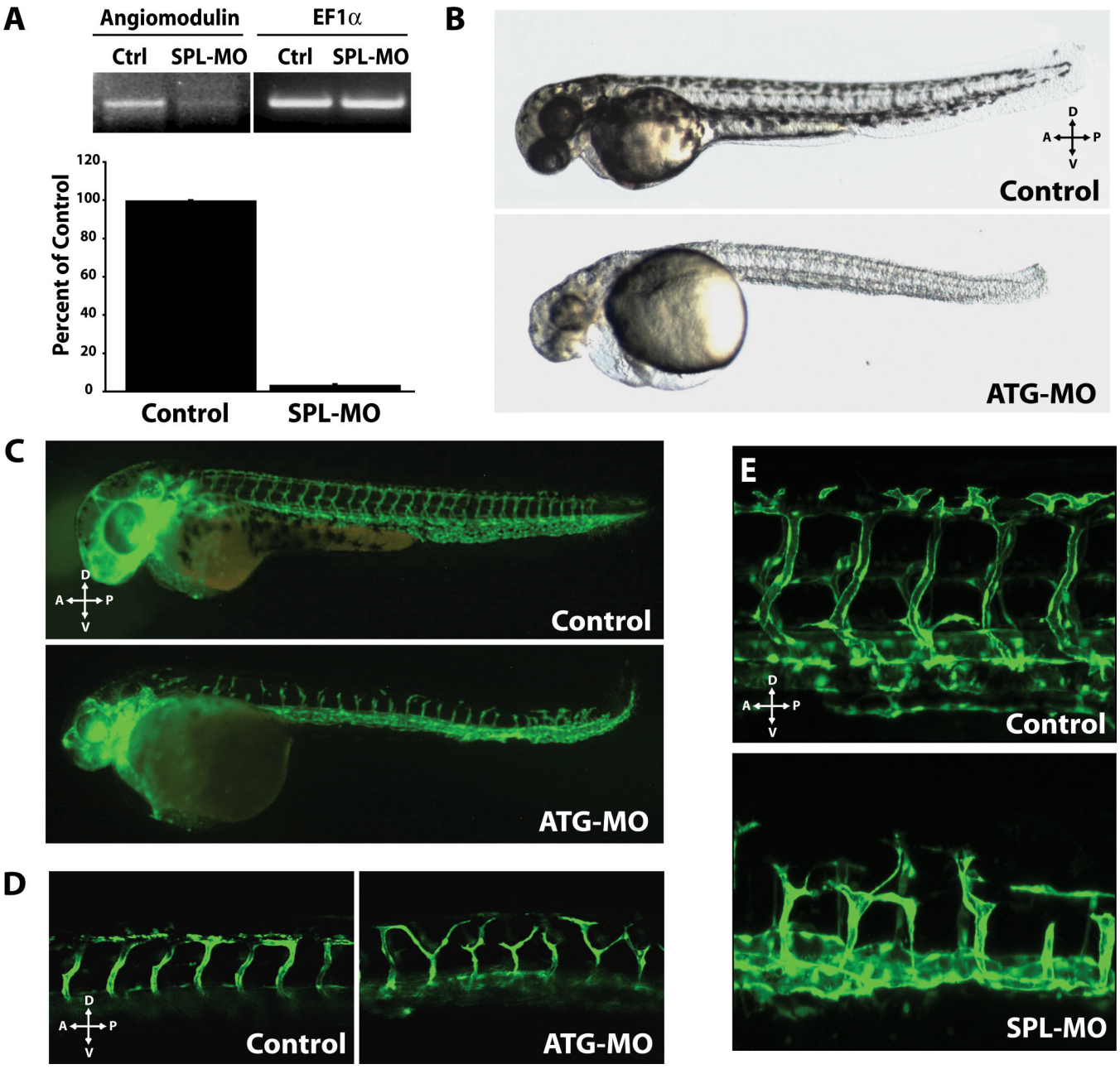

Figure 5. Knockdown of AGM results in a severe impairment in vascular patterning

A) Total RNA extracted from zebrafish injected with SPL-MO was assessed for AGM knockdown by RT-PCR and qPCR. SPL-MO resulted in a decrease of AGM mRNA to 5% of control. 24 hpf. B) Lateral views of 39 hpf control and AGM ATG-MO-injected embryos (ATGMO, 5 ng). The morphant phenotype manifests in pericardial edema and defects in yolk-extension, circulation, brain, and melanophores. 10 ng of ATG-MO produces a more severe phenotype. SPL-MO yielded similar phenotypes. C) 2.5 ng of ATG-MO injected in *fli1*:EGFP transgenic zebrafish embryos results in ISV defects. Axial vessels appear correctly specified. 48hpf. D) *fli1*:EGFP fish treated with 10ng ATG-MO or control MO demonstrating defect in ISV patterning. 56 hpf. E) 20ng of SPL-MO results in similar defects in ISV patterning. 48hpf.

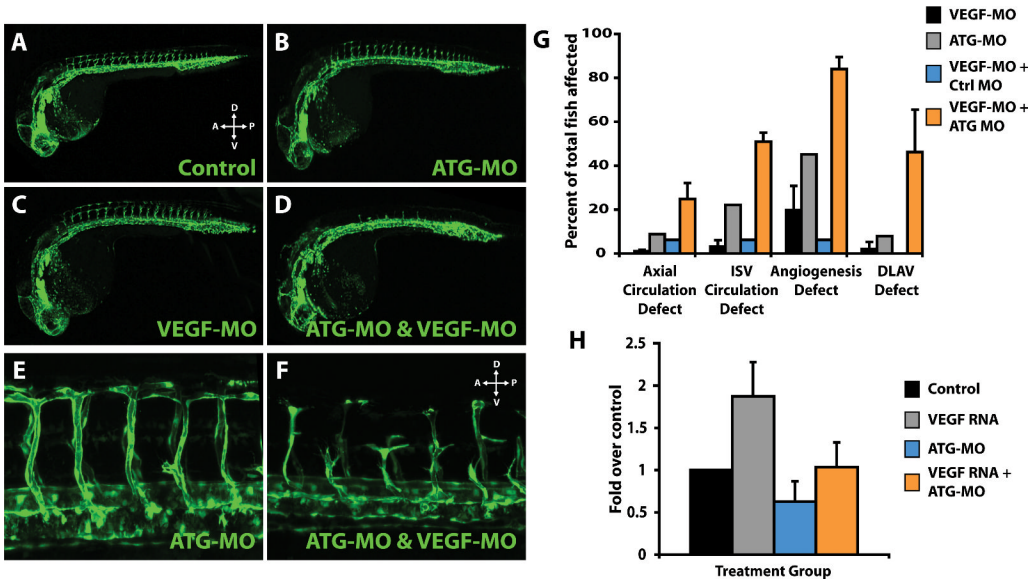

Figure 6. AGM interaction with the VEGF-A pathway is essential for proper patterning of nascent vessels

A-F) *fli1*:EGFP embryos were injected with (A) control MO; (B) subeffective dose ATG-MO at 0.5ng; (C) subeffective dose of VEGF-MO at 0.5ng; or, (D) ATG-MO and VEGF-MO at 0.5ng. Embryos were assessed for ISV angiogenesis at 24-28 hpf. Control, ATG-MO or VEGF-MO at subeffective doses resulted in minimal angiogenesis defects. ATG-MO & VEGF-MO injected simultaneously resulted in a robust decrease in angiogenesis and diminished sprouting in greater than 90% of the embryos at 24 hpf. Confocal micrographs of ISVs from control (E) or double-MO injected embryos (F) at 48 hpf. The sprouts that did form in a small number of the double-MO injected embryos were mispatterned and largely dysfunctional. G) Quantitation of defects in ATG-MO, VEGF-MO or combination MO-injected embryos as compared to controls at 48 hpf. Circulation defects in axial vessels or ISV, general angiogenesis defects, and defects in formation of the DLAV (including absent DLAV) were quantified by counting minimum of 30-100 embryos per group over a series of 3 independent experiments. Control MO injected embryos were normal. H) VEGF-A ($VEGF_{165/121}$) was overexpressed and compensatory expression of flk-1 was analyzed by qPCR. VEGF-A mRNA was injected alone or coinjected with ATG-MO into 20-50 embryos per group at the 1-2 cell stage. Total RNA was isolated at 24 hpf and qPCR was performed for flk-1. VEGF-A overexpression results in a two-fold increase in flk-1 expression; however, when co-injected with ATG-MO the compensatory increase in flk-1 is abrogated. *n=3*.

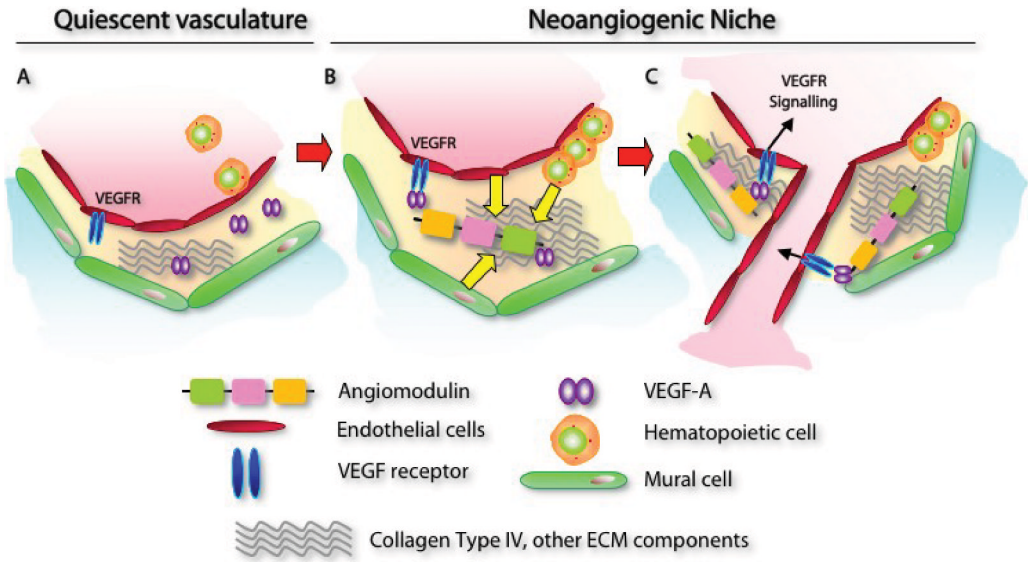

Figure 7. AGM regulates VEGF-A dependent neo-angiogenesis

A) In quiescent stabilized vasculature, VEGF-A will not actively signal through its receptors to induce angiogenesis. B-C) In the neoangiogenic niche, VEGF-A is required to rapidly signal through its receptors and transduce signals for cell proliferation, migration, orientation, patterning and survival. ECs, hematopoietic cells, and mural cells may secrete AGM into the neoangiogenic niche. AGM binds to collagen type IV and other extracellular matrix or basement membrane associated factors. AGM binds VEGF-A (B). AGM-mediated proper positioning of VEGF-A allows precise signaling via its receptors inducing effective angiogenesis (C).